Journal of Energy Storage 60 (2023) 106684

Contents lists available at ScienceDirect

Journal of Energy Storage

journal homepage: www.elsevier.com/locate/est

Research papers

Carbon footprint of Li-Oxygen batteries and the impact of material and structure selection

Melodie Chen-Glasser [a], Amy E. Landis [b], Steven C. DeCaluwe [c,*]

[a] Advanced Energy Systems Program, Colorado School of Mines, Golden, CO 80401, USA
[b] Department of Civil and Environmental Engineering, Colorado School of Mines, Golden, CO 80401, USA
[c] Department of Mechanical Engineering, Colorado School of Mines, Golden, CO 80401, USA

ARTICLE INFO

Keywords:
Carbon footprint
Li-O2 batteries
Materials selection

ABSTRACT

High energy density lithium-O_2 batteries have potential to increase electric vehicle driving range, but commercialization is prevented by technical challenges. Researchers have proposed electrolytes, catalysts, and binders to improve the battery capacity and reduce capacity fade. Novel battery design, however, is not always consistent with reduction in greenhouse gas (GHG) emissions. Optimizing battery design using solely electrochemical metrics ignores variations in the environmental impacts of different materials. The lack of uniform reporting practices further complicates such efforts. This paper presents commonly used lithium-O_2 battery materials along with their GHG emissions. We use LCA methodology to estimate GHG emissions for five proposed lithium-O_2 battery designs: (i) without catalyst, (ii) with catalyst, (iii) carbon-less and binder-less, (iv) anode protection, and (v) carbon-less, binder-less with gold catalyst. This work highlights knowledge gaps in lithium-O_2 battery LCA, provides a benchmark to quantify battery composition impacts, and demonstrates the GHG emissions associated with certain materials and designs for laboratory-scale batteries. Predicted GHG emissions range from 10–70 kg of CO_2 equivalent (kg CO_2e) kg^{-1} of battery, 60–1200 kg CO_2e kWh^{-1}, and 0.15–21 kg CO_2e km^{-1} of vehicle travel, if battery replacement is considered.

1. Introduction

Cheap, efficient, and high-energy density batteries will be critical in the drive to decarbonize the global energy sector, including passenger vehicles. Climate targets drive the transition to electric vehicles. Regulation (EU) 2019/631 sets emissions of passenger cars to 60 g CO_2 km^{-1} by 2030 and, in the United States, 40 CFR Parts 86 and 600 sets a target for fleet CO_2 to be 161 g mi^{-1} by 2026 [1,2]. Lithium-ion batteries are the predominant technology used for rechargeable energy storage, but the practical cell energy density for current intercalation-type chemistries is capped at around 200–225 Wh kg_{cell}^{-1} [3]. In battery electric vehicles (BEVs), this energy density is insufficient to provide driving range above 310 miles. Lithium oxygen (Li-O_2) batteries have been proposed to increase BEV driving range per charge, as they have a theoretical energy density comparable to gasoline, and experimental practical cell energy density as high as 1200 Wh kg_{cell}^{-1} on their first discharge cycle [4–6]. The lightweight and inexpensive air cathode could provide advantages over other energy storage solutions [7]. Energy density and chemical composition are key to new battery technologies, as they determine not only how much material is needed and how expensive building the battery will be, but the battery's lifecycle greenhouse gas (GHG) emissions. While much of next generation battery research address these climate targets, very few publications have quantified the GHG emissions to validate their results. With this in mind, Li-O_2 battery components should be analyzed in reference to their GHG emissions, in addition to electrochemical performance, to holistically evaluate a proposed storage technology's effectiveness in decarbonizing our energy economy.

A conventional Li-O_2 battery consists of a lithium metal anode, a porous separator, an electrolyte, and a carbon-based cathode (Fig. 1). The electrolyte consists of a solvent and lithium salt, and enables transport of Li^+ and oxygen (dissolved into the electrolyte from the gas feed). Li_2O_2 is formed at the interface between the electrolyte and the electronically-conductive carbon surface. The cathode is a mix of carbon particles attached to a current collector by a conductive polymeric binder. Variations on this design have been explored to improve performance. The cathode and electrolyte chemical composition and the associated cell potentials determine the nature and prevalence of parasitic reactions, mostly due to high reactivity of O_2^- intermediate species. Reactions between the O_2^- superoxide and cell components (such as the electrolyte or polymer binders) create deletrious co-products rather than forming Li_2O_2. Parasitic reactions passivate the electrode and

* Corresponding author.
E-mail address: decaluwe@mines.edu (S.C. DeCaluwe).

https://doi.org/10.1016/j.est.2023.106684
Received 29 October 2022; Received in revised form 20 December 2022; Accepted 9 January 2023
Available online 19 January 2023

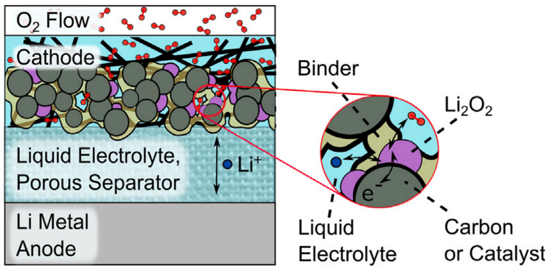

Fig. 1. A diagram of a conventional Li-O_2 Battery. Oxygen dissolves into the electrolyte from the gas feed, and diffuses into the cathode. There, it reacts with Li^+ ions, produced at the lithium anode, to create lithium oxides, such as Li_2O_2. The high theoretical energy density makes it a promising storage device for portable applications, such as battery electric vehicles.

degrade the battery components, leading to poor cycling. To eliminate these problems, researchers have experimented with a wide range of catalysts, electrolytes, and carbon materials [8–10].

Though decarbonizing the transportation sector is at the heart Li-O_2 battery research, their evolving design makes it difficult to draw conclusions about their ultimate climatic impact. As Li-O_2 batteries reach commercialization, their impact on the environment must be assessed, to ensure their implementation will have net environmental benefits. Life cycle analysis (LCA) and carbon footprinting (C-footprint) are ways to assign and compare possible environmental impacts between different designs and determine pathways for improvement. While purely electrochemical metrics such as gravimetric capacity, power density, and efficiency are critical benchmarks for environmentally benign energy storage technology, ultimately LCA provides the only path to judge the total environmental impact of a proposed technology. An efficient technology platform that is based on materials with high associated GHG emissions (due to material sourcing, transport, and/or processing) will likely always have deleterious environmental impacts, no matter its electrochemical performance.

Currently, few LCAs have been performed on Li-O_2 batteries. Moreover, current literature approaches have used disparate techniques to determine a representative Li-O_2 battery in their work [11–13]. Zackrisson et al. used an in-house experimental setup to provide the battery's mass inputs and performance predictions [11]. L. Wang et al. used the mass breakdown in Zackrisson et al.'s paper to compare Li-O_2, lithium-sulfur, and sodium-ion batteries [13]. This experiment-driven method has the benefit of being realistic, but only captures a fraction of the current Li-O_2 research. F. Wang et al. use BatPaC, a modeling software package from Argonne National Lab, to determine the material inputs required for a battery [12]. This modeling approach provides insight into the environmental impacts of a larger commercialized battery configuration and the potential of Li-O_2 batteries; however, its use of literature references to determine important properties differ from the materials assumed in the model, which makes it difficult to determine the accuracy of the reported C-footprint.

This paper provides the GHG emissions of materials commonly used in Li-O_2 batteries and applies LCA methodology to quantify the GHG emissions of five Li-O_2 batteries proposed in literature, representative of common experimental configurations. These include: (i) batteries without catalyst, (ii) batteries with catalyst, (iii) a carbon-less and binder-less battery, (iv) a battery with anode protection, and (v) a carbon-less, binder-less battery with precious metal catalyst. When compared with the results from two previous papers [11,12], the results present a benchmark range for projected GHG emissions, useful for comparison against other technology and future studies. Using this information, we can predict which materials will negatively impact the overall environmental impact of Li-O_2 batteries. In addition, we describe here how the lack of battery metric standards makes it difficult to perform LCA for GHG accounting and understand the true environmental impacts of new battery designs.

2. Experimental methods

This carbon footprint follows the LCA framework outlined in the ISO 14 040 series, which consists of four phases: goal and scope definition, life-cycle inventory (LCI) analysis, life-cycle impact assessment (LCIA), and interpretation [14]. In the goal and scope phase, the purpose of the study is clearly defined, allowing the appropriate system boundary and functional unit (FU) to be chosen. The system boundary clearly states what is included within the scope of the study, while the functional unit quantifies an output metric related to the study's purpose. The FU provides a way to determine the necessary quantities of input materials, which takes place during the LCI. The LCI is the process of determining which and how much of each material is needed to complete the LCA within system boundaries. In the LCIA, the emissions from these processes are interpreted with additional context through characterization factors, which normalize the environmental impact of chemicals into succinct categories, allowing comparison between difference processes. All of these steps are interdependent and should be iterated upon as the study is conducted. The data presented in this paper was collected from a wide range of literature sources, which are described in the Supporting Information (SI). The upstream emissions were determined using the ecoinvent 3.7.1 database [15] and the TRACI 2.1 method [16] was used for the LCIA, of which only GHGs are reported. TRACI uses IPCC 2001 global warming potential for chemicals with a 100-year time horizon [16]. The analysis presented herein compares five Li-O_2 battery designs proposed in previously published reports, summarized in Table 1. In addition, the results from two LCAs published by other authors are included, for comparison's sake.

Any given battery design contains a number design details; the five papers chosen here were done so based on their exploration of material impact and sufficiently descriptive methods sections to allow a rigorous and comprehensive analysis of GHG emissions. Where any gaps in the methods sections were encountered, papers and patents by the same research group were consulted to find necessary details. Xu et al., cover the impact of different electrolytes on the initial capacity of a Li-O_2 battery [17]. Marquez et al.'s work presents performance data for cells with different binders and catalysts [18]. The two papers by Asadi et al. (2016, 2018) provide examples of carbon-less, binder-less cathodes, with the more recent paper showing improvement after a change in electrolyte and addition of a protective anode coating [19,20]. Liu et al. provide an additional example of a carbon-less, binder-less cathode, with a precious metal catalyst [21]. Some of the materials examined in the paper are based on the components of the highlighted batteries. In addition, other materials commonly mentioned in literature were examined to provide a wider range of GHG emissions for different battery components [8–10]. The final selected materials were determined using an overlap between common materials and previously determined synthesis pathways, which are explained fully in the SI.

2.1. Goal, scope, functional units, and system boundary

The primary goal of this paper is to correlate commonly used Li-O_2 battery materials with their associated GHG emissions and calculate the overall GHG emissions for Li-O_2 battery designs presented in the literature. The data and analysis presented are used to examine the variability in Li-O_2 battery emissions, demonstrating how predictions vary with different FU. In conjunction, this work seeks to increase use of LCA as a primary tool during the battery design process. We provide a comprehensive list of LCI data for common materials, for adoption by others in the field, and recommendations to make LCA more convenient for a broader range of battery researchers.

The scope of an LCA determines the system boundary and its level of detail. Historically, battery LCAs have presented information for different scopes, which result in data being reported in different FU, as shown in Fig. 2 [22]. In cradle-to-gate studies, the scope spans from the resource extraction to their exit from the factory gate, but excludes

Table 1
Papers whose experimental or LCA data are referenced in this study. The § symbol indicates a previous LCA study whose results are adopted and reproduced for comparison/benchmarking purposes. The 'Abbreviation' column describes how each paper is referenced throughout the manuscript, for brevity's sake.

Ref:	1*st Author*	Description	Abbreviation
[11]	Zackrisson§	A published LCA, which used their own lab scale experiments to do an LCA	Lab Scale LCA§
[12]	Wang§	A published LCA, which used BatPaC to get weight percentages for their design	BatPaC LCA§
[17]	Xu	A battery with no catalyst and varied electrolytes. This paper does not have extended cycling data	Electrolyte Var.
[18]	Márquez	Batteries with varied catalysts and varied binders, cycled up to 20 times.	Cat. Binder Var.
[19]	Asadi	A carbon-less, binder-less battery with MnO2 catalyst, and ionic liquid as electrolyte cycled 50 times.	Carbon/binder-less
[20]	Asadi	A carbon-less, binder-less battery with MnO2 catalyst, and ionic liquid as electrolyte, and an anode protective layer, cycled 500 times.	Anode protection
[21]	Liu	Carbon-less, binder-less cathode with gold catalyst, cycled up to 200 times.	Gold Cat.

any emissions related to their use or end-of-life. For this study, the FU of 1 kg of battery and 1 kWh of battery capacity serve as metrics for the cradle-to-gate scope which can be applied to experimental studies that do not report extended cycling data. A cradle-to-grave boundary includes the use and end-of-life of the battery, in addition to the other previously mentioned processes. For this study, a cradle-to-grave LCA is performed for papers which reported metrics relating to capacity fade. A BEV is assumed to travel 200,000 km during its lifetime and the FU is 1 km. For these, data or assumptions regarding battery lifetime and degradation with extended cycling are required. This concept is demonstrated in Fig. 2.

2.1.1. C-footprint assumptions and limitations

A complete process flow diagram (PFD), for the battery featured in Asadi et al. (2016) is shown in Fig. 2, and provides an example of the system boundary applied for each paper. The steps labeled in red—related to solvent mixing, cooling systems, and car manufacturing details—have been excluded from the process. In addition, battery recycling, deflagaration as a result of vehicle accident, and projected changes in environmental policy that might impact energy mix are considered beyond the scope of this study. More information on these topics, and why they are excluded is presented in the SI.

The amount of oxygen required for battery operation was calculated using the battery capacity, as described in the supplementary information (SI). The ecoinvent database was then used to determine the environmental impacts associated with that component. If the component was not found in ecoinvent, the component's LCI was traced from another paper until processes were available. Electricity use was sourced from the mix from Guandong, China, where many battery factories are currently located; details of this mix are given in SI Table 35 [23]. All assembled components were assumed to travel 2000 km by rail and 1000 km by truck [12]. The battery manufacturing energy was assumed to be 74 MJ kg_{bat}^{-1}, with 42% of that energy being attributed to natural gas and the rest to electricity [11,24]. Both natural gas and electricity are used in the battery process. For example, dry rooms, the moisture-free rooms required for battery manufacturing, typically consume energy from both sources [25].

The energy consumed during battery charging, E_{use}, is calculated using Eq. (1), whose variables are defined and values provided in Table 2 [12]. A battery lifetime of 200,000 km is used to determine the electricity consumed over the battery lifetime. The vehicle driving range of 300 km per charge is assumed as the industry average, corresponding to a battery capacity of roughly 46.6 kWh [26]. The GHG emissions per kg of battery and per kWh of energy recovered from the battery are calculated using Eq. (2), using the specific gravimetric capacity reported in the research paper. The GHG emissions for the battery are determined by Eq. (2), where m_i refers of to the mass of material i required to build the battery, $GHG_{sp,i}$ refers to the specific emissions of material i on a per-unit-mass basis, C_{sp} refers to the experimentally-measured gravimetric specific capacity (kWh kg^{-1}) of the battery, and C_{tot} is the total battery capacity (kWh). The mass basis used to report experimental specific capacity (per kg active material or per kg of total battery mass) is not always explicitly stated, requiring assumptions during the C-footprinting. These are explained in detail in the SI. According to the United States Advanced Battery Consortium (USABC), batteries need to be replaced when the capacity decreases by 20%, and replacement should be factored into the LCA [27].

Table 2
Variable definitions and assigned values for Eq (1).

Variable	Units	Definition	Value
T	km	Total driving distance	200,000
x_{cycle}	km	Cycle driving distance	300
$E_{\text{discharged}}$	kWh	Battery capacity	46.6
η_{charger}	–	Efficiency of charger	0.90
η_{battery}	–	Efficiency of the battery	Battery specific

$$E_{\text{use}} = \frac{E_{\text{discharged}}}{x_{\text{cycle}}\eta_{\text{charger}}\eta_{\text{battery}}}T \quad (1)$$

$$GHG_{\text{tot,bat}} = \frac{\Sigma_i m_i GHG_{sp,i}}{\Sigma_i m_i}\frac{C_{\text{tot}}}{C_{\text{sp}}} \quad (2)$$

2.2. Life cycle inventory

LCI refers to the collection of information essential for completing the LCA. This includes determining the mass of each material input for battery fabrication, as well as the energy associated with its sourcing/extraction, transport, and processing. The methods sections of the $Li\text{-}O_2$ battery papers referenced in Table 1 provide inputs for the mass inventory [17–21]. In addition, other popular materials are selected from literature reviews and included in the LCI to identify materials with high GHG emissions [8–10]. Fig. 3 shows the GHG emissions associated with different battery components. The process for determining the mass inventories of each battery is included in the SI. In many cases, these materials are not available directly in the ecoinvent database. The process for synthesizing these components, as well as their representative ecoinvent process are listed in the SI as well.

2.2.1. Electrolyte components

The $Li\text{-}O_2$ battery electrolyte is typically comprised of two components: an O_2-soluble, aprotic solvent and a lithium salt. The electrolyte shuttles lithium ions between the anode and cathode and facilitate transport of O_2 between the gas flow channel and the carbon–electrolyte interface where charge transfer occurs in the cathode (see Fig. 1). In some cases, additives are included to promote or prevent certain electrolyte reactions and improve transport properties.

Solvent GHG emissions per unit mass are presented in Fig. 3a. Solvents make up a large percentage of the battery mass; their GHG emissions are therefore important. Common solvents used in $Li\text{-}O_2$ batteries have included carbonates, amides, sulfones, nitriles, ethers, and ionic liquids [10]. Most organic solvents have known decomposition pathways in the presence of O_2^- reaction intermediates. The binder and catalyst choices both influence parasitic reactions occurring in solution [18,28]. While ionic liquids are more stable, they often have lower ionic conductivity and O_2 solubility, resulting in reduced performance at higher currents [17]. These disadvantages can be partially addressed *via* solvent mixtures or cathode compositions that maximize $\pi-\pi$ bonds between ions and the surface [29]. Solvent mixtures, such as methyl nonafluorobutyl ether (E7100), are also employed to reduce the solvent

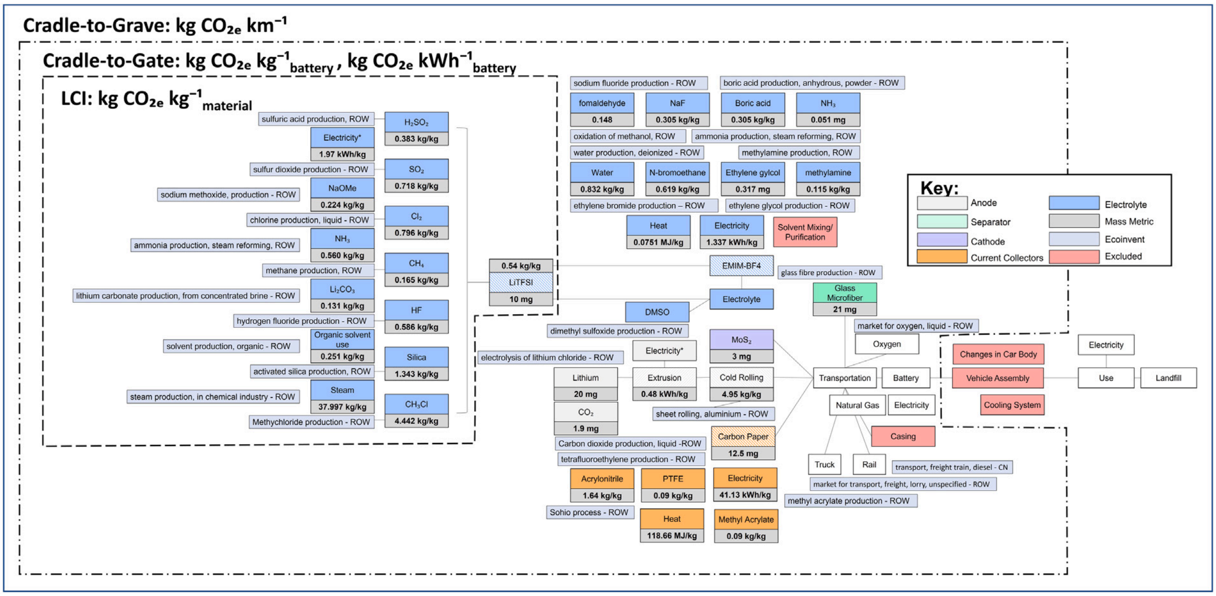

Fig. 2. The process flow diagram for battery assembly, with relevant processes in ecoinvent. The units established here are adopted throughout the paper.

flammability or increase oxygen solubility [10]. As seen in Fig. 3a, most solvent GHG emissions range from 1–15 kg CO_2e $kg^{-1}_{material}$, making them good candidates. The two ionic liquids, BMIM-C4mim and EMIM-BF4 have a slightly higher GHG emissions compared to other common solvents. An exception to this is E7100, which will be discussed in conjunction with other fluoropolymers.

GHG emissions for salts and other additives are presented in Fig. 3b. The detailed LCI for these materials is found in SI Tables S7–S13. In Fig. 3b, solutes with typically higher concentrations (0.5M–1M in solution) are marked in blue, while species present at levels around 0.1M are considered additives and are marked in red. $LiNO_3$ has functioned as both an electrolyte salt and additive. Additives can serve as redox mediators (RM), O_2 carriers, and solid–electrolyte interface (SEI) stabilizers. Typically, potassium and lithium iodide (KI & LiI) are added as RM [30,31], while boric acid (BA) and tetraethyl orthosilicate (TEOS) have been explored as SEI stabilizers [32]. $LiNO_3$ promotes SEI formation, as well as being an RM [8,33,34]. Organic additives such as small amounts of polyethylene glycol, polyvinylidene fluouride (PvDF), and complex fluoropolymers have been examined in the context of improving O_2 transport [10,29,35].

Fluorocarbons such as E7100 and perfluorotributylamine (PFTBA) have higher global warming potentials compared to other materials, and can also degrade the ozone layer. The GHG emissions of E7100 were estimated at 2973 kg CO_2e $kg^{-1}_{material}$, with the bulk of the GHG emissions attributed to an assumption that 1% is admitted to the atmosphere during manufacturing [36]. A single molecule of PFTBA released to the atmosphere is equivalent to 7100 molecules of CO_2 in terms of greenhouse gas equivalence [37]. The use of fluoropolymers as electrolytes and additives must be justified by sufficient reduction in the mass or increased longevity and efficiency of the battery.

2.2.2. Cathode materials

Catalysts (Fig. 3c), binders (Fig. 3d), and carbon materials (Table 3) are the three most commonly discussed cathode material classes. The catalysts used in Li-O_2 batteries includes pure metals, metal oxides, peroxides, metal organic frameworks, and composite materials [8]. Catalysts can be added to decrease the voltage gap between the charge and discharge potentials, or to increase the battery capacity. Reducing the voltage gap typically prevents some parasitic reactions and reduces the charging voltage, both of which reduce emissions in the use phase. Among these, the materials in Fig. 3c have received particular attention, with manganese dioxide and cobalt oxide being the most popular. The LCI for these are available in SI tables S114–S118.

Catalyst GHG emissions range from 2–70,000 kg CO_2e $kg^{-1}_{material}$. Catalyst emissions fall into two distinct groupings, with precious metal catalyst emissions exceeding those for other choices by orders of magnitude. In most laboratory-scale batteries, catalysts usage is on the order of mg cm^{-2}, which translates to g kg^{-1} in a commercialized battery. Non-precious metal catalyst emissions are typically below 15 kg CO_2e $kg^{-1}_{material}$.

Much like electrolytes, binders are prone to degradation when exposed to the O_2^- superoxide. Many initial Li-O_2 designs used PvDF, a common lithium-ion battery binder, but more recent batteries use materials such as polytetrafluoroethylene (PTFE), polyvinylpyrrolidone (PVP), polyethylene oxide (PEO), or polyethylene (PE), which are less prone to O_2^- attack. Though these materials reduce the amount of deleterious byproducts, they occlude reaction sites by preventing electron transport, limiting the battery capacity [38]. Li-Nafion has been explored as a conductive binder to address this problem [39,40].

Fig. 3d presents the specific GHG emissions for common binder materials, which range from roughly 2–140 kg CO_2e $kg^{-1}_{material}$. The detailed LCI for these components are available in SI tables S19–S22. Fluoropolymers once again tend to have a higher GHG emissions than alternatives, although their use as binders has significant beneficial impact on the cycling and the capacity of the battery. Recently, binderless cathodes have received attention. These may provide greater stability, but may require higher value materials such as carbon nanotubes or gold, and typically result in lower capacity due to loss of electrochemically active surface area [41]. LCA would be a useful tool to analyze the trade-offs between capacity, capacity fade, and materials choice when considering binderless Li-O_2 batteries.

Finally, carbon is a material that often makes up highest volume percentage of the cathode and provides the majority of reactive area for Li_2O_2 product formation. Carbon reacts with Li_2O_2 during charging over 3.5 V. Some researchers address this through novel catalysts to reduce the charging potential, while others attempt to eliminate carbon entirely [41]. Often, Li-O_2 battery cathodes are composed of carbon-binder slurries, which are dried into disks. Some of these dried slurries contain catalysts or are pressed onto current collectors. Many Li-O_2 batteries use some type of carbon black in their electrode, such as

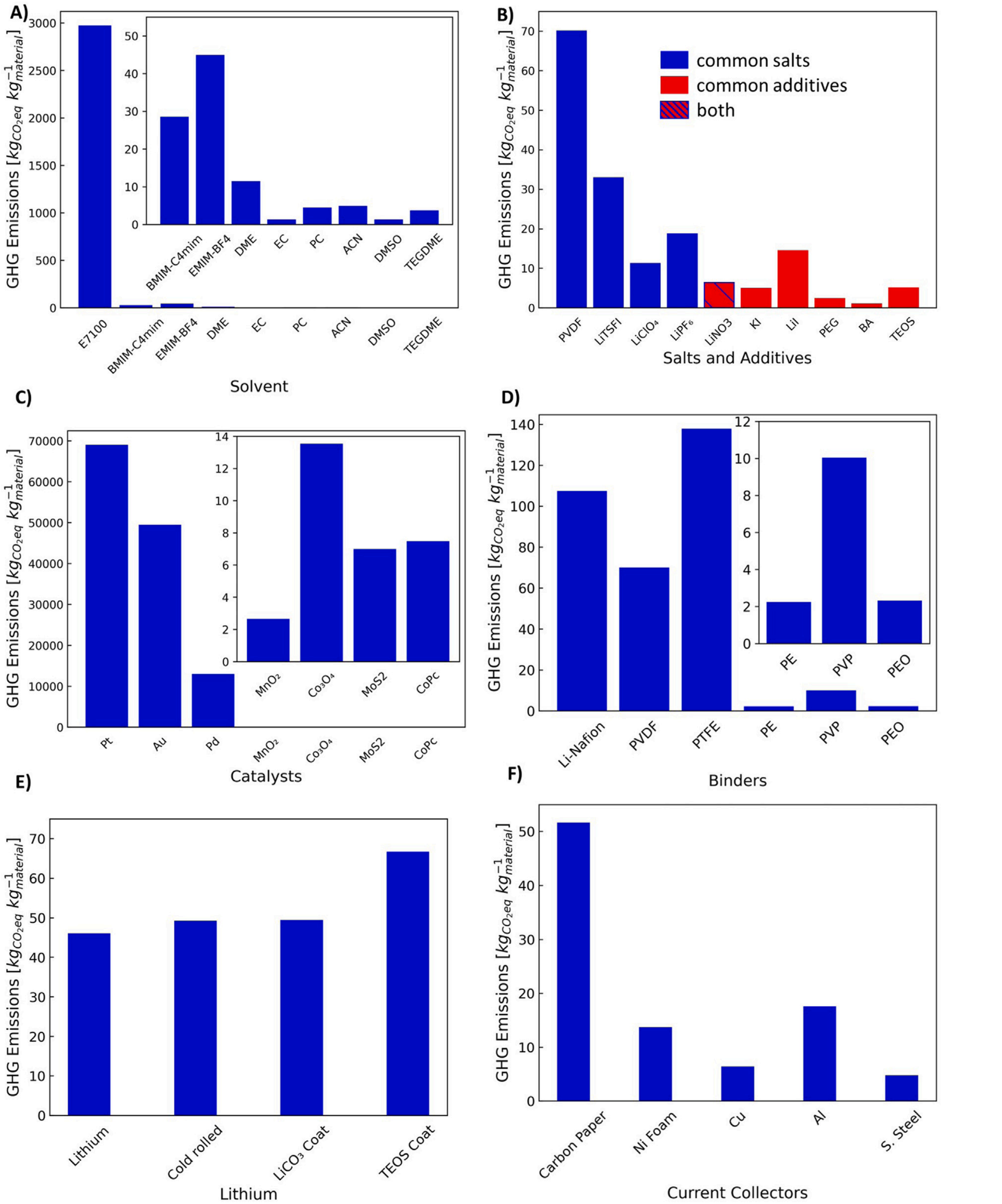

Fig. 3. GHG emissions of commonly used Li-O_2 battery materials: (a) solvents, (b) salts/additives (c) catalysts, (d) binders, (e) lithium, and (f) current collectors. (For interpretation of the references to color in this figure legend, the reader is referred to the web version of this article.)

Ketjen Black, acetylene black or Vulcan. These are typically modeled as generic carbon black in the ecoinvent database [42]. Other carbon materials, include graphene, graphene oxide, or carbon nanotubes (CNTs), have ranges for their GHG emissions depending of their synthesis pathways, as summarized in Table 3 [8]. To correctly account for these materials, the production pathway should be determined. CNTs produced by chemical vapor deposition on a fluidized bed, the most common method, emit 480 kg CO_2e $kg^{-1}_{material}$ [43,44].

2.2.3. Current collectors

Li-O_2 batteries can have current collectors at the anode and cathode to assist electron transport. Fig. 3f shows the specific GHG for common

Table 3
Typical GHG emissions for carbon cathode materials.

Material	GHG (kg CO_2e $kg^{-1}_{material}$)	Ref
Carbon black	1.8	[15]
Graphene	430–620	[45]
Graphene Oxide	53–208	[45]
Carbon nanotubes	480–28,500	[44]

current collector materials. Copper is typically used at the anode, while the other materials shown in Fig. 3f are used at the cathode [34,46]. The cathode current collector stability is another subject of considerable Li-O_2 battery research. Carbon paper is a popular current collector as it adds reactive surface area; however, as previously mentioned, carbon materials can degrade at high voltage. Nickel foam is similarly constrained; cycling potentials should be limited to between 2.0 and 4.0 V [46]. Nickel foam can be used for binderless cathodes, as it provides a porous structure for catalyst deposition or growth and Li_2O_2 deposits [47,48]. Of the current collectors presented, carbon paper with 95% PTFE coating has the highest associated GHG emissions.

2.2.4. Lithium anode

Typically, Li-O_2 batteries use pure lithium foil as the anode. If the thickness of this lithium is on the order of mm, it has been extruded from ingots. Between 0.75–0.4 mm, it has undergone some sort of cold rolling. Additional cold-rolling can reduce the Li thickness further, to as low as 0.04 mm. The surface of the lithium can be treated with TEOS to improve resistance to lithium dendrites [49]. The lithium can also be treated with CO_2 to create a protective coating of 5 μm of Li_2CO_3 [50]. The differences in GHG emissions between these processing steps can be seen in Fig. 3e, which shows little variation between different processing or coating methods. The detailed LCI can be found in SI tables S30–S33.

2.3. Sensitivity analysis

Sensitivity analysis elucidates how values and assumptions in the LCI affect the overall LCA results. Below, we present two sensitivity analyses:

1. Varying manufacturing energy (MJ per kg of battery fabricated). Two previous LCAs for Li-O_2 batteries each used a single value for the energy required to manufacture lithium-ion batteries. However, energy consumption estimates of a cell assembly plant can range between 35 MJ kg^{-1}_{bat} to 400 MJ kg^{-1}_{bat}, depending on whether the plant is operating at full capacity [25].
2. Exploring different use phase electricity sources based on region. Given an EV's dependence on grid energy, regional impacts are examined by different grid energy mixes. The baseline case uses a grid mix in China, given the large size of their BEV fleet. Other mixes from Norway, India, the United States, and South Africa were chosen to examine the impacts of global adoption. The grid from Norway was selected due the high per capita adoption of BEVs there [51], while India has one of the highest projected growth rates in BEV adoption [52]. Finally, the potential for BEV development in South Africa is explored, given its relatively high ratio of EV equipment to EV [53]. Table S35 shows the breakdown of the energy mixes for each country, based on ecoinvent 3.7 data [15].

3. Results and discussion

Fig. 4 shows the mass and GHG percentages attributed to different battery components for six different designs reported in the literature and summarized in Table 1[11,12,17–19,21]. For all six batteries, the lithium anode is less than 20% of the mass, but can be responsible for a much larger percentage of the GHG emissions. In the case of Wang et al. and Zackrisson et al. (BatPac LCA and Lab Scale LCA in Fig. 4, respectively), this is accentuated by the fact that ecoivent has recently changed the GHG emissions associated with lithium production from roughly 167 to 46 kg CO_2e $kg^{-1}_{lithium}$ [11,12].

Examining the GHG emissions attributed to different battery components highlights design considerations to reduce GHG emissions and demonstrates the challenges inherent in reducing emissions for Li-O_2 batteries. In many cases, reducing the amount of lithium through approaches such as so-called 'anode-free' batteries would have a noticeable impact on the GHG emissions [54]. In the case of Zackrisson et al. [11] and Liu et al. [32], even though the cathode makes up a very small mass percentage of the battery, GHG-intensive cathode materials mean that the cathode accounts for a significant portion of the battery's GHG emissions. For Liu et al., the high GHG material in the cathode is gold nanoparticles. In Zackrisson et al.'s work, the cathode is comprised of Co_2O_3 particles and CNTs; however, the materials data reported in that publication provides insufficient detail to determine the specific cause of the high GHG emissions. Liu et al. uses a binderless, carbonless cathode, where Au loading is 0.22 mg cm^{-2}, leading to a very small percentage of active material present on the current collector. Reducing the GHG by reducing catalyst loading while retaining its positive performance impacts would be challenging. Continued research into Au nanoparticle catalysts may therefore be unlikely to produce an Li-O_2 battery with net positive GHG impacts.

In most of the batteries in Fig. 4, the electrolyte constitutes a large percentage of the battery mass, but typically a smaller percentage of the GHG emissions. The 'Carbon/binder-less' study from Asadi et al. is an exception. Their electrolyte mass fraction is lower, but due to use of an ionic liquid electrolyte solvent, it represents the largest contribution to the battery's GHG emissions [19]. These preliminary findings only relate to the allocation of GHG emissions by mass (kg CO_2e kg^{-1}_{bat}). Selecting an electrolyte with higher GHG emissions can be worthwhile if it improves the overall capacity, charging efficiency, or capacity fade of the battery enough to compensate for its per-unit mass GHG emissions.

Cradle-to-grave GHG emissions for five different batteries are shown in Fig. 5. The GHG emissions for production and use range from 0.15 to 0.6 kg CO_2e km^{-1}, and jump to roughly 24 kg CO_2e km^{-1} when battery replacement is considered. Currently, internal combustion engine vehicle GHG emissions range from 0.1–0.2 kg CO_2e km^{-1}, and Li-ion battery EVs operating in China range from 0.1–0.15 kg CO_2e km^{-1}, according to one study [55]. Current Li-O_2 batteries require additional advances to be competitive, from an environmental standpoint. Furthermore, in Europe, GHG emission targets are 0.095 kg CO_2e km^{-1}, with an additional 37.5% reduction by 2030 (0.06 kg CO_2e km^{-1}) [1].

Battery replacement effects draw attention to a key difficulty in Li-O_2 materials research: cycling efficiency. So far, Li-O_2 battery LCA studies have assumed that these batteries will last the vehicle lifetime (200,000 km is assumed here); however, this ignores how gains in cycling efficiency reduce the overall GHG emissions. In addition, from this sample of batteries, carbon-less, binder-less batteries have increased cycling efficiency, but also increased GHG emissions. Future research should focus on better understanding this trade-off. Finally, the comparison between carbon/binder-less [19] and anode-protective [20] shows the impacts from continued improvement of a single design, reinforcing the importance of design iteration. Although their design is not competitive with commercialized lithium-ion batteries, at present, both the production and replacement GHG emissions decrease significantly between the two studies. Associating decreases in GHG emissions with experimental practice is another way to quantify successful avenues of research.

The relative impacts of battery production vs. use on GHG emissions varies between the six studies. In the C-footprint results for Cat. Binder Var. [18] and BatPaC LCA§ [12], the BEV use phase results in the highest contribution to GHG emissions. In these cases, GHG emission

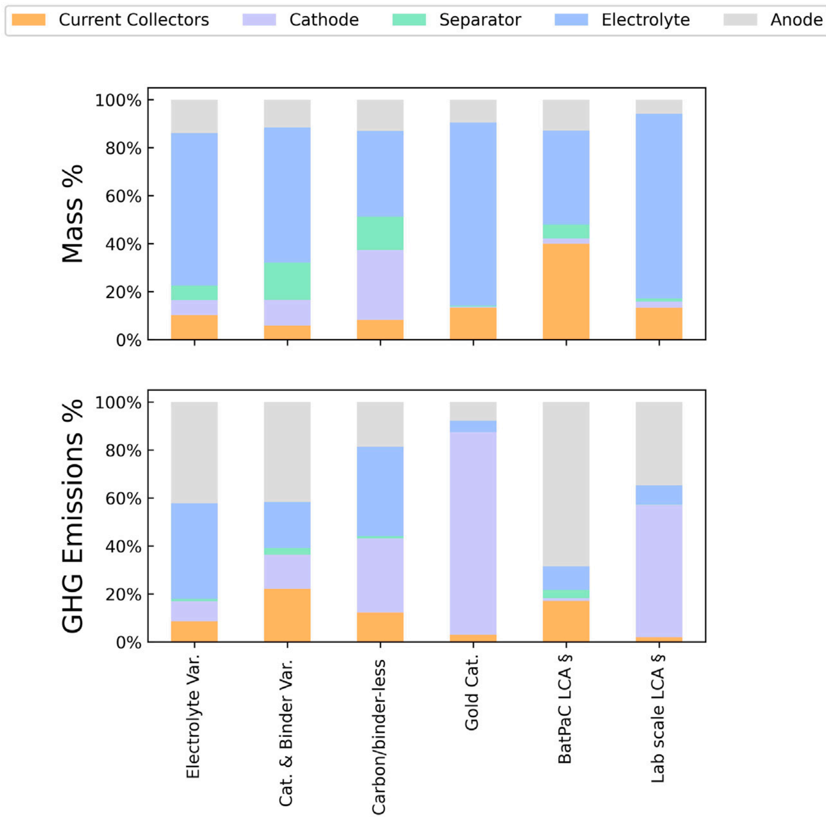

Fig. 4. The mass and GHG emissions breakdown of six Li-O_2 battery designs proposed in the literature: Electrolyte Var. [17], cat & binder var, [18], carbon/binderless [19], gold cat [32], BatPaC LCA, [12], and Lab-scale LCA [11]. The § symbol indicates a previous LCA study whose results are adopted and reproduced for comparison/benchmarking purposes.

can be reduced by improving the cycling efficiency of the battery or improving the energy mix. The round-trip energy efficiency of Li-O_2 batteries ranges from 50%–70%, while for lithium-ion batteries it is closer to 80% [56]. The impact of efficiency can be seen by comparing the results from Cat. Binder Var. [18], which has an efficiency of 68%, to those from Carbonless/Binderless [19,20], where efficiency is closer to 85%. Following from Eqs. (1) and (2), increasing cycling efficiency by 10% corresponds to a roughly 10% reduction in grid GHG emissions (Figure S4).

The Carbon/binderless, Anode Protection and Gold Cat. batteries [19,20,32] demonstrate conditions where the majority of GHG emissions are associated with production phase. The ‘Lab Scale LCA’ study assumes a European energy mix, which decreases the use case emissions [11]. In Eq. (2), the total mass of materials needed for battery production depend on the capacity/sizing of the battery. The ‘Lab Scale LCA’ reports a specific capacity that is an order of magnitude higher than the ‘Anode Protection’ battery [11,20], yet they have similar GHG emissions, indicating that the GHG emissions of the Lab Scale LCA§'s components are likely higher, per unit mass [11,19,20]. This demonstrates that material choices play a large role in determining whether capacity improvements actually lead to GHG emission reductions.

3.1. The material impact on cycling and capacity

Fig. 6a shows the GHG emissions on per unit mass and energy bases. GHG emissions from the five papers reviewed here range between 10–80 kg CO_2e kg_{bat}^{-1} or as much as 120 kg CO_2e kg_{bat}^{-1} if the manufacturing energy is toward the upper end of the estimated range (error bars represent sensitivity analysis due to variations the manufacturing energy). Lithium-ion battery GHG emissions are estimated to be from 1.7–8.1 kg CO_2e kg_{bat}^{-1}, however have a much lower gravimetric capacity than Li-O_2 batteries. The large range in gravimetric capacities for Li-O_2 batteries makes comparing them on a per unit energy basis more convenient. Comparing the Electrolyte Var. [17] and Cat & Binder Var. [18] studies, the GHG emissions associated with a battery on a mass bases have little impact on the GHG emissions on a kWh basis. These papers use both binder and carbon components to increase their surface area, leading to high variation in capacities. In contrast, the Carbon/Binder-less, Anode Protection, and Gold Cat. batteries all have binder-less carbon-less cathodes [19,20,32]. They originally report their capacities on a $kg_{\mathrm{active\ material}}$ basis rather than reporting them on a kg_{cell} basis. Here, they are shown to have the highest associated GHG emissions, which translates to their cradle-to-grave emissions in the previous section (see Fig. 5). The battery capacity plays an essential role in the lifetime GHG emissions of the battery and determines the battery mass needed for production.

In Fig. 6b, the GHG emissions kWh_{bat}^{-1} are plotted against the battery capacity, showing the importance of reporting capacity on a kg_{cell} basis, rather than a $kg_{\mathrm{active\ material}}$. It is worth noting that in Fig. 6, the batteries with lower capacities due to their lack of surface area (Carbon/Binder-less, Anode Protection, and Gold Cat. [19,20,32]) have much higher cycling efficiency, which brings down their GHG emissions on a per vehicle km basis, but increases their production emissions. This trade-off should be given more rigorous evaluation. If binder-less, carbon-less Li-O_2 batteries are preferable in terms of life-cycle GHG emissions because they offer reduced capacity fade, but ultimately have less gravimetric capacity or higher GHG emissions on a cell basis, then their development should not be labeled as environmentally beneficial. This discovery gives a pathway forward for future research, which should focus on either increasing the surface area of binder-less, carbon-less batteries, or on decreasing reactivity and cell degradation in the presence of binders and carbon.

LCA offers another method to pre-select materials for further study, as shown in Fig. 6c. Here, various raw materials in the Cat & Binder Var.

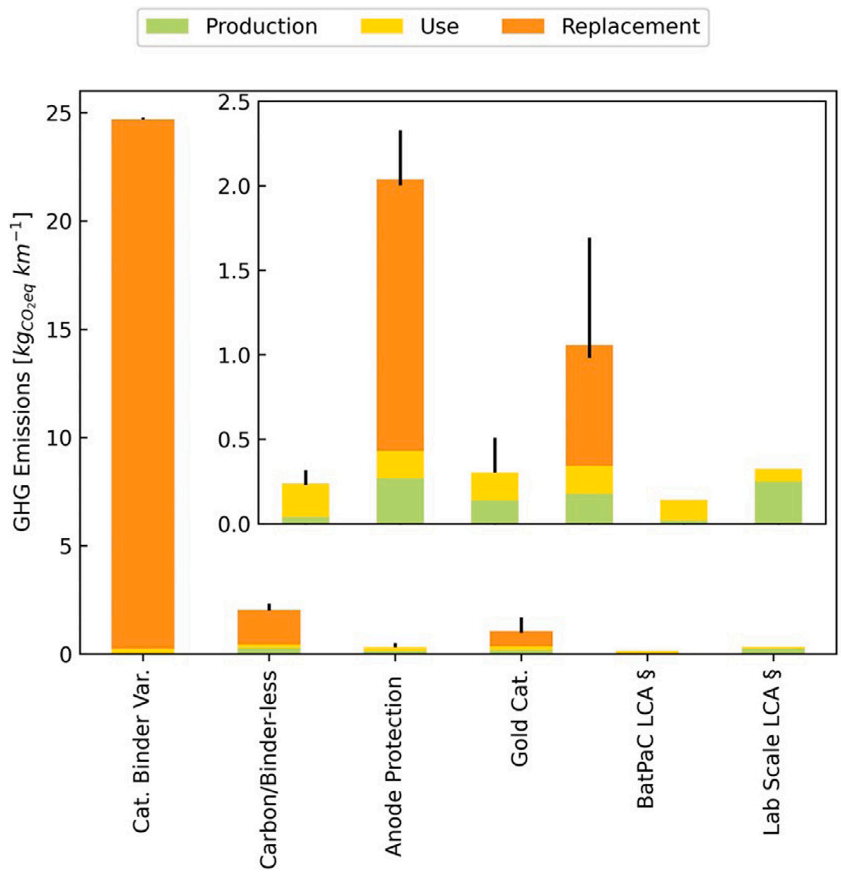

Fig. 5. The cradle-to-grave GHG emissions for six batteries: cat & binder var, [18], carbon/binderless [19], anode protection [20], gold cat [32], BatPac LCA§ [12], and Lab-scale LCA§ [11]. In this graph, the error bars represent uncertainty of manufacturing energy. The inset removes the 'replacement' emissions from 'Cat. Binder Var'. and re-scales to provide greater resolution of the remaining elements. The § symbol indicates a previous LCA study whose results are adopted and reproduced for comparison/benchmarking purposes.

design are substituted with high-GHG carbon, electrolyte, or catalyst materials [18]. In their study design, the catalysts have the same mass loading (mg cm^{-2}) and the slurry composition is determined by weight ratio. C-footprinting can add another dimension to experimental design, where in addition to comparing battery capacity, cycling efficiency, or voltage potential gap, GHG emissions are used to identify promising research directions.

As an example, if CNT were substituted for carbon by weight, the battery capacity would have to increase around 500 Wh kg_{cell}^{-2} for their added GHG impacts to be negated by capacity increase. Given that other papers have report capacities of 1200 Wh kg_{cell}^{-2} as previously mentioned, this would be challenging but not impossible. However, a platinum catalyst would have to increase battery capacity to 6000 Wh kg_{cell}^{-2}, which is beyond the theoretical capacity of Li-O_2 batteries, 3505 Wh kg_{cell}^{-1} [57]. In this case, the cathode catalyst mass must be reduced, or an alternative non-precious catalyst must be identified.

Capacity is, of course, not the only driving factor for catalyst selection. Many researchers use catalysts to prevent degradation or improve battery efficiency. As an example, the impacts of platinum are translated to the use phase in Fig. 6d, where the impacts of replacement are shown. Using Carbon/Binderless [19] and Cat &Binder Var [18] as examples and replacing the MnO_2 catalyst with an equal mass of platinum or the electrolyte solvent with E7100 to eliminate the need for replacement of the battery doubles the resulting the GHG emissions. In the case of Carbon/Binderless [19], the battery should be replaced 7 times during the lifetime of the battery, while the capacity fade of Carbon/Binderless [19] is much higher and the battery needs to be replaced after each use. If platinum catalysts could reduce capacity fade, the total GHG emissions would still greatly exceed targets made by the EU and would not be competitive with lithium-ion batteries. These scenarios are rough examples of how GHG emissions calculations could be used to guide battery design and future R&D.

Incorporating C-footprinting throughout the battery design process can therefore provide significant benefits, but will require updates to our reporting practices. Product Category Rules (PCRs) for next generation batteries could be developed to make the data collection and reporting consistent, such that comparisons among new battery technologies and materials are also consistent [58]. This may build on previous battery PCRs, where special attention is given to the high variation in capacities and materials [59]. Many methods sections in the literature report battery components using inconsistent metrics; the electrolyte is reported as a volume; catalysts on a mass per area basis, and current collectors and lithium as an area. However in databases such as ecoinvent, most GHG metrics are given on a mass basis. More reporting on mass measurements of electrolyte components, current collector meshes, and lithium weight would facilitate C-footprinting or LCA in parallel with experimental research. As researchers investigate novel components, such as ionic liquids or catalysts, for using in Li-O_2 batteries, their GHG emissions should be evaluated in tandem.

3.2. Sensitivity analysis

Sensitivity analysis provides another means of identifying research and development avenues with potential for high impact in GHG reductions. Throughout the paper, GHG emissions variation due to uncertainties in manufacturing energy is shown via error bars on graphs. This wide range of values shows the importance of enhancing the precision of energy estimates for Li-O_2 battery manufacturing, which

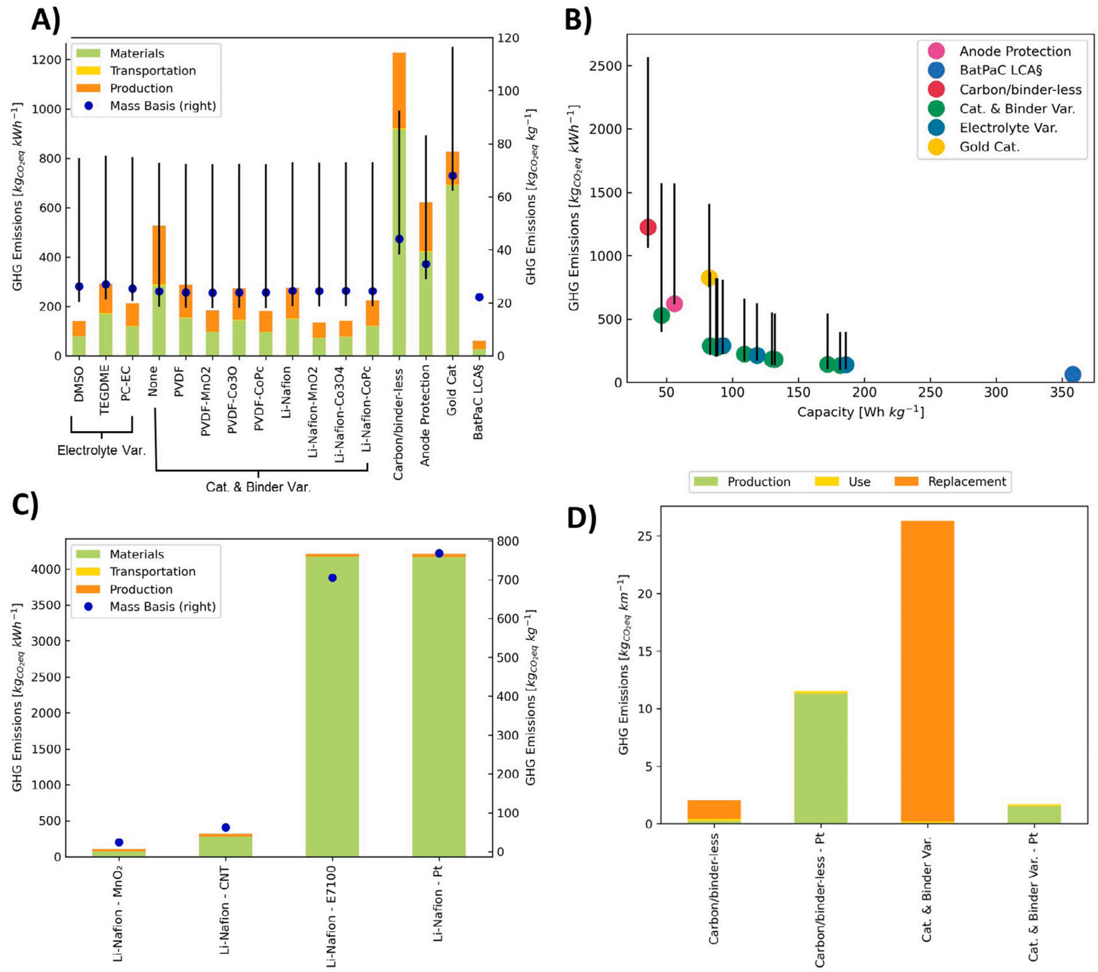

Fig. 6. Cradle-to-grave GHG sensitivity to battery design variables. (a) The GHG emissions on per unit mass and energy bases, where error bars reflect sensitivity to uncertainties in manufacturing energy. (b) GHG emissions per unit energy plotted against battery specific capacity (c) the impact of replacing materials in the 'Cat & Binder Var.' study (left-hand side) with high GHG emission materials, and (d) the impact of replacing the catalyst mass in two studies ('Carbon/Binderless' and 'Cat &B inder Var') with Pt, reported per km of vehicle travel.

are currently unavailable due to lab scale assembly of Li-O_2. Because specific manufacturing energy is given in units of MJ kg^{-1}, the total manufacturing energy scales with battery mass and is therefore highly depended on battery's specific capacity (Wh kg^{-1}). GHG emissions for lower specific capacity batteries are highly sensitive to the specific manufacturing energy, highlighting the need for accurate specific manufacturing energy estimates. Future work might examine the impact of more sophisticated manufacturing energy models to predict the energy required for high- and low-throughput manufacturing approaches [25].

Fig. 7 presents C-footprint results for the carbon-/binder-less battery as a function of the energy mix during the use phase. The impacts of different energy mixes are presented relative to the base case, which uses China's electricity grid. Battery GHG emissions are relatively comparable for China and the USA. For both countries, coal is the major contributor to almost every metric, despite the fact that coal accounts for 25% of USA's electricity but 75% of China's. The major difference here is that China uses hard coal, while the USA uses more lignite. 91% of the energy in South Africa's grid comes from coal, while 98% of Norway's electricity comes from hydroelectric power, giving them the highest and lowest GHG emissions, respectively.

This sensitivity analysis shows that while grid emissions cause significant variation in lifecycle GHG emissions, reducing grid emissions to near zero will still fall short of current lithium-ion battery emission targets or European standards, as the production-phase emissions are still quite high. Closer examination of Norway's results shows that use-phase GHG emissions are negligible compared to the production or replacement GHG emissions. While it is true that Li-O_2 batteries are still in a low-technology-readiness stage, researchers often mention their development will be have positive environmental impacts, but focus their efforts on increasing battery capacity or cycling efficiency, rather than decreasing net emissions. Battery researchers cannot control grid emissions, but can tailor their experiments by selecting and focusing materials that reduce emissions during battery production. Reductions in production-phase emissions on a commercial scale can have significant impact, and will become even more important for continued GHG emission reductions as grids de-carbonize.

4. Conclusions

Currently, there are very few C-footprint studies or LCA for Li-O_2 batteries; the LCAs available provide widely varying results. This work presents detailed life-cycle inventory data and resulting C-footprinting results for a range of proposed Li-O_2 battery designs. Our results show that the material choice and resulting properties, such as capacity and cycling efficiency, greatly change the GHG emissions. Quantifying GHG emissions provides researchers with another tool to assess how material choices impact the technology's production and use phase emissions. However, the diversity in proposed Li-O_2 materials makes it difficult to predict the environmental impacts of Li-O_2 batteries upon commercialization. We recommend accurate documentation and reporting of data relating to electrolyte volume, separator density, oxygen consumption, and mass distribution of catalysts to provide higher quality data for

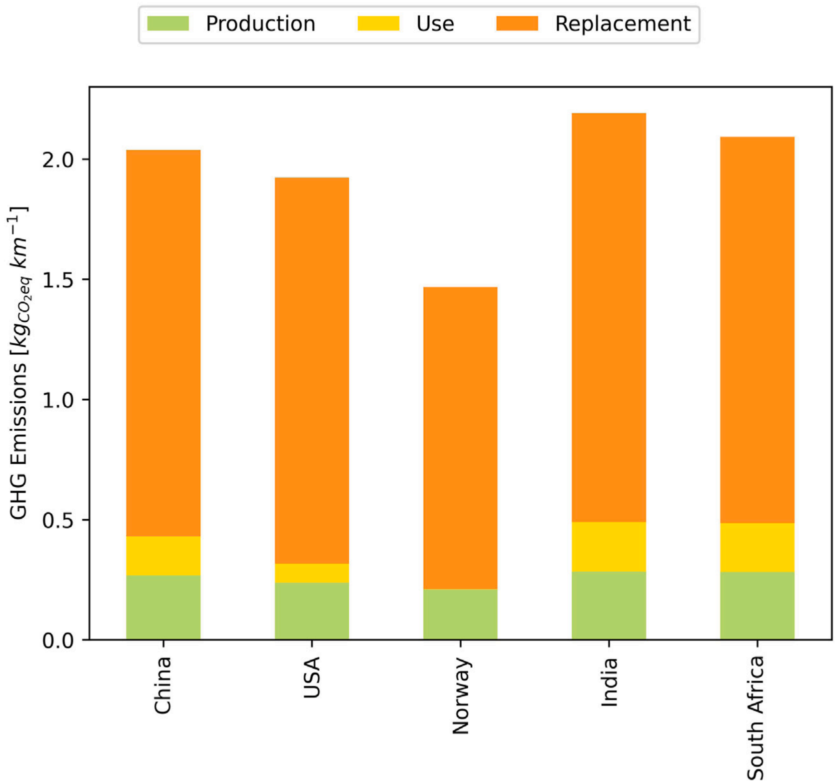

Fig. 7. Carbon emission sensitivity to grid energy mix for the carbon/binder-less battery. GHG emissions are presented per km of vehicle travel. [19].

LCA. Often, these data are inconsistently reported or altogether missing from experimental descriptions, hindering attempts to understand environmental impacts of proposed battery designs. In particular, the inconsistent manner in which researchers present capacity makes it difficult to compare between studies. The capacity should be reported in Wh kg^{-1}_{cell}, instead of $kg^{-1}_{active\ material}$, as this is the relevant metric for cradle-to-grave LCA.

Furthermore, we have demonstrated via C-footprint prediction and analysis that evaluating the GHG emissions on a per mass basis, while necessary for future calculations, is not sufficient to identify the battery's climate impacts, and that reporting on a per unit energy basis is preferable for holistically evaluating battery design. In most cases the GHG emissions kg^{-1} battery are not good indicators for the actual GHG emissions over the battery lifetime. When materials with high specific GHG emissions are used, their electrochemical benefits are limited, because of upper theoretical limits to capacity and efficiency. In particular, precious metal catalysts, such as Pt or Au, have 3–4 orders magnitude higher GHG emissions than some of their non-precious counterparts. As researchers explore new battery designs, they should use GHG emissions to guide material selection and experimental design, in order to achieve the ultimate goal of reducing environmental impacts and producing batteries that are competitive with lithium-ion batteries on an environmental basis.

5. Abbreviations

boric acid - BA
battery electric vehicle - BEV
electric vehicle - EV
function unit - FU
Greenhouse gas - GHG
perfluorotributylamine - PFTBA
process flow diagram - PFD
redox mediators - RM
solid–electrolyte interface - SEI
supplementary information - SI
tetraethyl orthosilicate - TEOS
Life Cycle Analysis – LCA
life cycle inventory – LCI
Life cycling inventory assessment- LCIA
lithium iodide - LI
Lithium-oxygen - Li-O_2
methyl nonafluorobutyl ether - E7100
potassium iodide - KI
product category rules - PCR

CRediT authorship contribution statement

Melodie Chen-Glasser: Conceptualization, Writing – original draft, Investigation, Data curation. **Amy E. Landis:** Methodology, Validation, Resources, Writing – review & editing. **Steven C. DeCaluwe:** Validation, Writing – review & editing, Supervision, Funding acquisition.

Declaration of competing interest

The authors declare that they have no known competing financial interests or personal relationships that could have appeared to influence the work reported in this paper.

Data availability

The data that has been used is confidential.

Funding

Financial support provided by US National Science Foundation, Award 1 903 440, Program Manager Dr. Raymond Adomaitis

Appendix A. Supplementary data

Supplementary material related to this article can be found online at https://doi.org/10.1016/j.est.2023.106684.

References

[1] CO_2 Emission Performance Standards for Cars and Vans, European Commission, 2022, https://ec.europa.eu/clima/eu-action/transport-emissions/road-transport-reducing-co2-emissions-vehicles/co2-emission-performance-standards-cars-and-vans_en. Accessed: 2022-09-25.

[2] US Enivronmental Protection Agency, Revised 2023 and later model year Light-duty vehicle greenhouse gas emissions standards, Fed. Reg. 86 (283) (2021) 74434–74526.

[3] D.L. Wood III, J. Li, C. Daniel, Prospects for reducing the processing cost of Lithium ion batteries, J. Power Sources 275 (2015) 234–242.

[4] G. Zhang, S. Lu, S. Zhao, L. Zhang, H. Sun, Revealing the local cathodic interfacial chemism inconsistency in a practical large-sized Li–O_2 model battery with high energy density to underpin its key cyclic constraints, ACS Appl. Mater. Interfaces 13 (20) (2021) 23853–23685.

[5] A.C. Lim, H.J. Kwon, H.C. Lee, D.J. Lee, H. Lee, H.J. Kim, D. Im, J.G. Seo, Mechanically reinforced-CNT cathode for Li-O_2 battery with enhanced specific energy via ex situ pore formation, Chem. Eng. J. 385 (2020) 123841.

[6] Y.S. Cho, H. Kim, M. Byeon, Y. Jung, D. Lee, J. Park, H.J. Kown, H. Lee, M. Kim, W. Choi, D. Im, C.R. Park, One step "growth to spinning" of biaxially multilayered CNT web electrode for long cycling Li–o_2 batteries, Carbon 182 (2021) 318–326.

[7] A. Rinaldi, Y. Wang, K. Tan, O. Wijaya, R. Yazami, Lithium-air batteries for medium and large-scale energy storage, in: Advances in Batteries for Medium and Large-Scale Energy Storage, 2015, pp. 387–440.

[8] Z. Ma, X. Yuan, L. Li, Z.-F. Ma, D.P. Wilkinson, L. Zhang, J. Zhang, A review of cathode materials and structures for rechargeable Lithium–air batteries, Energy Environ. Sci. 8 (2015) 2144–2198.

[9] J.-W Jung, S.-H. Cho, S.N. Jong, I.-D. Kim, Current and future cathode materials for non-aqueous Li-air (O_2) battery technology – A focused review, Energy Storage Mater. 24, 512–5528.

[10] J. Lai, Y. Xing, N. Chen, L. Li, F. Wu, R. Chen, Electrolytes for rechargeable Lithium–air batteries, Angew. Chem. Int. 59 (8) (2020) 2974–2997.

[11] M. Zackrisson, K. Fransson, J. Hildenbrand, G. Lampic, C. O'Dwyer, Life cycle assessment of Lithium-air battery cells, J. Clean. Prod. 135 (2016) 299–311.

[12] F. Wang, Y. Deng, C. Yuan, Life cycle assessment of Lithium oxygen battery for electric vehicles, J. Clean. Prod. 265 (2020) 121339.

[13] L. Wang, J. Hu, Y. Yu, K. Huang, Y. Hu, Lithium-air, Lithium-sulfur, and sodium-ion, which secondary battery category is more environmentally friendly and promising based on footprint family indicators? J. Clean. Prod. 276 (2020) 124244.

[14] ISO 14040 international standards, in: Environmental Management-Life Cycle Assessment: Principles and Framework, International Organization for Standardization, Geneva, Switzerland, 2006.

[15] G. Wernet, C. Bauer, B. Steubing, J. Reinhard, E. Moreno-Ruiz, B. Weidema, The ecoinvent database version 3 (part I): overview and methodology, Int. J. Life Cycle Assess 21 (9) (2016) 1218–1230.

[16] J. Bare, Tool for the Reduction and Assessment of Chemical and Other Environmental Impacts (TRACI) version 2.1 User's Guide, US EPA Office of Research and Development, Washington, DC, 2014.

[17] W. Xu, J. Hu, M.H. Engelhard, S.A. Towne, J.S. Hardy, J. Xiao, J. Feng, M.Y. Hu, J. Zhang, F. Ding, M.E. Gross, J.-G. Zhang, The stability of organic solvents and carbon electrode in nonaqueous Li-O_2 batteries, J. Power Sources 215 (2012) 240–247.

[18] P. Márquez, J. Amici, M.J. Aguirre, F. Herrera, C. Francia, S. Bodoardo, Synergic effect of catalyst/binder in passivation side-products of Li-oxygen cells, J. Solid State Electrochem. 23 (2019) 3309–3317.

[19] M. Asadi, B. Kumar, C. Liu, P. Phillips, P. Yasaei, A. Behranginia, P. Zapol, R.F. Klie, L.A. Curtiss, A. Salehi-Khojin, Cathode based on molybdenum disulfide nanoflakes for Lithium–oxygen batteries, ACS Nano 10 (2) (2016) 2167–2175.

[20] M. Asadi, B. Sayahpour, P. Abbasi, A.T. Ngo, K. Karis, J.R. Jokisaari, C. Liu, B. Narayanan, M. Gerard, P. Yasaei, A. Mukherjee, K.C. Lau, R.S. Assary, F. Khalili-Araghi, R.R. Klie, C.A. Larry, A. Salehi-Khojin, A Lithium–oxygen battery with a long cycle Life in an air-like atmosphere, Nature 555 (2018) 502–206.

[21] S. Liu, G. Wang, F. Tu, J. Xie, H.Y. Yang, S. Zhang, T. Zhu, G. Cao, X. Zhao, Au-nanocrystals-decorated δ-MnO_2 as an efficient catalytic cathode for high-performance Li–O_2 batteries, Nanoscale 7 (2015) 9589–9596.

[22] J. Sadhukhan, M. Christensen, An in-depth Life cycle assessment (LCA) of Lithium-ion battery for climate impact mitigation strategies, Energies 14 (17) (2021) 5555.

[23] S. Wu, S. Pen, X. Zhang, D. Wu, T.Zhang Luo Wei, S. Zhou, G. Yang, H. Wan, L. Wu, Levels and health risk assessments of heavy metals in urban soils in Dongguan, China, J. Geochem. Explor. 148 (2015) 71–78.

[24] M. Zackrisson, Lars Avellán, J. Orlenius, Life cycle assessment of Lithium-ion batteries for plug-in hybrid electric vehicles – critical issue, J. Clean. Prod. 18 (15) (2010) 1519–1529.

[25] J. Dunn, L. Gaines, J.C. Kelly, K. Gallagher, The significance of Li-ion batteries in electric vehicle Life-cycle energy and emissions and recycling's role in its reduction, Energy Environ. Sci. 8 (2014) 158–168.

[26] W. Kempton, Electric vehicles: Driving range, Nature Energy 1 (2016) 16131.

[27] P. Marques, R. Garia, L. Kulay, F. Freire, Comparative Life cycle assessment of Lithium-ion batteries for electric vehicles addressing capacity fade, J. Clean. Prod. 229 (2019) 787–794.

[28] H. Geaney, C. O'Dwyer, Examining the role of electrolyte and binders in determining discharge product morphology and cycling performance of carbon cathodes in Li-O_2 batteries, J. Electrochem. Soc. 163 (2) (2015) 43.

[29] M. Balaish, A. Kraytsberg, Y. Ein-Eli, A critical review on Lithium–air battery electrolytes, Phys. Chem. Chem. Phys. 16 (2014) 2801–2822.

[30] H. Zhang, G.G. Eshetu, X. Judez, C. Li, L.M. Rodriguez, M. Armand, Electrolyte additives for Lithium metal anodes and rechargeable Lithium metal batteries: Progress and perspectives, Angew. Chem. Int. Ed. 57 (46) (2018) 15002–15027.

[31] I. Landa-Medrano, M. Olivares-Marín, G. Bergner, R. Pinedo, A. Sorrentino, E. Pereiro, I.Ruiz de Larramendi, J. Janek, T. Rojo, D. Tonti, Potassium salts as electrolyte additives in Lithium–oxygen batteries, J. Phys. Chem. C 121 (7) (2017) 3822–3829.

[32] T. Liu, J.P. Vivek, E.W. Zhao, J. Lei, N. Garcia-Araez, C.P. Grey, Current challenges and routes forward for nonaqueous Lithium–air batteries, Chem. Rev. 120 (14) (2020) 6558–6625.

[33] W. Li, H. Yao, K. Yan, G. Zheng, Z. Lian, Y.-M. Chiang, Y. Cui, The synergetic effect of Lithium polysulfide and Lithium nitrate to prevent Lithium dendrite growth, Nature Com 6 (2015) 7436.

[34] Q. Li, Z. Shoupu, Y. Lu, 3D porous cu current collector/Li-metal composite anode for stable Lithium-metal batteries, Adv. Funct. Mater. 27 (18) (2017) 1606422.

[35] A.A. Uludağ, H. Akbulut, M. Tokur, H. Algül, T. Çetinkaya, M. Uysal, Stability effect of some organic and inorganic additions in the EMITFSI–LiTFSI nanocomposite electrolytes for Lithium air batteries, Microsyst. Technol. 22 (2016) 953–963.

[36] M. Weckert, Comparative Life cycle assessment of CFC-replacement compounds in different technical applications, 2008.

[37] University of Toronto, New long-lived greenhouse gas discovered: Highest global-warming impact of any compound to date, ScienceDaily (2013).

[38] G.-E. Park, H.T. Le, H.-S. Kim, P.N. Didwal, C.-J. Park, Mn/Co oxide on Ni foam as a bifunctional catalyst for Li–air cells, Ceram. Int. 46 (12) (2020) 20335–20344.

[39] Z. Wen, C. Shen, Y. Lu, Air electrode for the Lithium–air batteries: Materials and structure designs, ChemPlusChem 80 (2) (2015) 270–287.

[40] H. Cheng, K. Scott, Improving performance of rechargeable Li-air batteries from using Li-Nafion® binder, Electrochim. Acta 116 (2014) 51–58.

[41] A. Luntz, B. McCloskey, S. Gowda, H. Horn, V. Viswanathan, Cathode electrochemistry in nonaqueous Lithium air batteries, in: The Lithium Air Battery, Fundamentals, Springer, 2014, pp. 56–120.

[42] Y. Liang, J. Su, X. Beidou, Y. Yu, D. Ji, Y. Sun, C. Cui, J. Zhu, Life cycle assessment of Lithium-ion batteries for greenhouse gas emissions, Resour. Conserv. Recycl. 117 (2017) 285–293.

[43] A. Eatemadi, H.Karimkhanloo Daraee, M. Kouhi, N. Zarghami, A. Akbarzadeh, M. Abasi, Y. Hanifehpour, S.W. Joo, Carbon nanotubes: properties, synthesis, purification, and medical applications, Nanoscale Res. Lett. 9 (1) (2014) 393.

[44] H.Y. Teah, T. Sato, K. Namiki, M. Asaka, K. Feng, S. Noda, Life cycle greenhouse gas emissions of long and pure carbon nanotubes synthesized via on-substrate and fluidized-bed chemical vapor deposition, ACS Sustain. Chem. Eng. 8 (2020) 1730–1740.

[45] M. Cossutta, J. McKechnie, S.J. Pickering, A comparative LCA of different graphene production routes, Green Chem. 19 (2017) 5874–5884.

[46] X. Liu, D. Wang, S. Shi, Exploration on the possibility of Ni foam as current collector in rechargeable Lithium-air batteries, Electrochim. Acta 87 (2013) 865–871.

[47] Q.-C. Zhu, S.-M. Xu, Z.-P. Cai, M.M. Harris, K. Wang, J.-S. Chen, Towards real Li-air batteries: A binder-free cathode with high electrochemical performance in CO_2 and O_2, Energy Storage Mater. 7 (2017) 209–215.

[48] L. Li, A. Manthiram, Decoupled bifunctional air electrodes for high-performance hybrid Lithium-air batteries, Nano Energy 9 (2014) 94–100.

[49] Y. Deng, J. Li, X. Gao, C. Yaun, Life cycle assessment of Lithium sulfur battery for electric vehicles, J. Power Sources 343 (2017) 284–295.

[50] A. Salehi-khojin, M. Asadi, B. Sayahpour, P. Abbassi, M. Gerard, Protected anodes and methods for making and using same, 2017, US Patent US20200058927A1.

[51] M.A. Aasness, J. Odeck, The increase of electric vehicle usage in Norway—incentives and adverse effects, Eur. Transp. Res. Rev. 7 (2015) 34.

[52] World Energy Outlook 2014, International Energy Agency, Paris, France, 2014.

[53] Global EV Outlook 2021, International Energy Agency, Paris, France, 2021, https://www.iea.org/reports/global-ev-outlook-2021. Accessed: 2022-09-25.

[54] S. Park, D. Jun, G. Lee, S. Lee, Y. Lee, Toward high-performance anodeless batteries based on controlled Lithium metal deposition: a review, J. Mater. Chem. A 9 (2021) 14656–14681.

[55] J. Woo, H. Choi, J. Ahn, Well-to-wheel analysis of greenhouse gas emissions for electric vehicles based on electricity generation mix: A global perspective, Transp. Res. D 51 (2017) 340–350.

[56] A. Eftekhair, Energy efficiency: a critically important but neglected factor in battery research, Sustain. Energy Fuels 1 (2017) 2053.

[57] P.G. Bruce, S. Freunberger, L.J. Hardwick, J.M. Tarascon, Li–O_2 and Li–S batteries with high energy storage, Nature Mater. 11 (2012) 12–26.

[58] ISO 14045 international standards, in: Environmental Labels and Declarations — Type III Environmental Declarations — Principles and Procedures, International Organization for Standardization, Geneva, Switzerland, 2006.

[59] RECHARGE, PEFCR - product environmental footprint category rules for high specific energy rechargeable batteries for mobile applications, 2020.